4-1-1999

Resonant Oscillation of a Liquid Metal Column Driven by Electromagnetic Lorentz Force Sources

Sergey N. Makarov
Worcester Polytechnic Institute, makarov@wpi.edu

Reinhold Ludwig
Worcester Polytechnic Institute, ludwig@wpi.edu

Diran Apelian
Worcester Polytechnic Institute, dapelian@wpi.edu

Resonant oscillation of a liquid metal column driven by electromagnetic Lorentz force sources

Sergey Makarov, Reinhold Ludwig,[a] and Diran Apelian
Metal Processing Institute, Department of Mechanical Engineering, Worcester Polytechnic Institute, Worcester, Massachusetts 01609-2280

(Received 21 July 1998; revised 24 November 1998; accepted 11 January 1999)

In this paper, a theoretical study is conducted in order to establish the feasibility of a liquid metal acoustic resonator (liquid gallium or liquid aluminum) for high-amplitude acoustic oscillations. The fundamental resonant frequency typically lies between 5 and 40 kHz. The oscillations are induced by an alternating Lorentz force density applied directly to the liquid metal volume. Depending on the boundary conditions, two different resonator types (open–closed and open–open) are theoretically investigated. The analysis incorporates the effects of impedance termination, volume absorption, wall friction, acoustic radiation from the open end, and nonlinear inflow–outflow losses. The actual elasticity of the container, either a ceramic or quartz tube, and the coupled solid–liquid interactions are taken into consideration. Based on this investigation, theoretical predictions are conducted for the quality factor and the pressure level for the liquid metal resonator under various geometric and boundary conditions. They indicate that resonant amplitudes of 10–20 atm can be achieved using commercially available high-current audio amplifiers. © *1999 Acoustical Society of America.* [S0001-4966(99)03104-5]

PACS numbers: 43.35.Bf, 43.35.Zc, 43.20.Ks, 43.25.Gf, 43.38.Ar, 43.38.Dv [HEB]

LIST OF SYMBOLS

a	tube radius [m]
$\mathbf{B}$, B	magnetic flux density [Wb/m^2=Tesla]
$B/A=n-1$	nonlinearity parameter of the liquid
c_0	sound speed in the liquid metal [m/s]
c_l	longitudinal wave speed in the termination/tube material [m/s]
c_p	phase velocity of compressional waves in a elastic plate [m/s]
c_p	specific heat at constant pressure [J/kg K]
E	Young's modulus of the termination/tube material [GPa]
$\mathbf{f}$, f, $\hat{f}$	Lorentz force density and its complex amplitude [N/m^3]
f_n	driving force density for nth resonance [N/m^3]
F	total Lorentz force [N]
F_n	total driving force for nth resonance [N]
h	wall thickness of the container [m]
$\mathbf{i}, i_x$	current density [A/m^2]
I, $\hat{I}$	total current (not rms!) and its complex amplitude [A]
j	imaginary unit
k_1, k_{1n}	wave number of the driving force [1/m]
K	circumferential stiffness of the tube wall [N/m^3]
L	height of the liquid metal column [m]
p, p_0	acoustic pressure and ambient pressure, respectively [Pa]
P	pressure amplitude of resonant oscillations (at antinode) [atm, Pa]
Q	quality factor of the resonator
$\mathbf{r}, \mathbf{r}_0$	observation point and source location point, respectively
S	tube cross-section [m^2]
w	velocity of the liquid metal in z direction [m/s]
x,y,z	Cartesian coordinates [m]
$Z_s=\rho_s c_l$	termination acoustic impedance [kg/m^2 s]
α	semi-empirical loss factor for inflow–outflow losses
α/f^2	sound absorption coefficient [s^2/m]
β	thermal expansion coefficient at constant pressure [1/K]
η	radial displacement of the tube wall [m]
η_s	shear viscosity of the liquid metal [Pa s]
η_e	effective shear viscosity of the liquid metal [cf. Eq. (1)] [Pa s]
θ	polar angle (xy-plane)
κ	thermal conductivity of the liquid metal [J/(m s K)]
λ	acoustic wavelength [m]
μ_e	effective kinematic viscosity (η_e/ρ_0) of the liquid metal [m^2/s]
ν	Poisson's coefficient of the termination/tube material
ρ_0	density of the liquid metal [kg/m^3]
ρ_s	density of the termination/tube material [kg/m^3]
ρ_l	resistivity of the liquid metal [Ω m]
ω	angular frequency [1/s]

INTRODUCTION

Acoustic resonators are valuable tools for collecting small inclusions in various fluids at nodes (anti-nodes) due to

[a]Also at Electrical and Computer Engineering Department, Worcester Polytechnic Institute, Worcester, MA 01609-2280.

the exerted acoustic radiation force.[1–3] The intense acoustic field can increase the wettability of solid inclusions in a liquid metal[4] and thus facilitate their deposition on the sensor surface. This makes acoustic standing waves an attractive mechanism from the viewpoint of sensor development for processing small inclusions in molten metals. Detection of small nonmetallic inclusions residing in a metallic melt (aluminum) has received increased attention due to industrial demand for the manufacturing of high quality metal products.[5–7]

To induce high-amplitude resonant oscillations of a liquid metal column, two problems have to be investigated. The first is related to the excitation force. Standard piezoelectric excitation becomes cumbersome under high-temperature conditions. Guided buffer rods and special coolers are necessary to transmit the pressure wave to the melt.[8–10] Alternatively, excitation methods based on electromechanical resonance show good performance, but they are restricted to one fixed frequency.[1]

The second problem pertains to the high acoustic impedance of the liquid metal, typically 6–9 times greater than the impedance of water. If a buffer rod is used as a transmitting element, its acoustic impedance is within the same order of magnitude. Therefore, no effective reflection from the driven end is created. This condition considerably limits the oscillation amplitude of a piezoelectric resonator. In practice, it is difficult to achieve good acoustic reflection from *any* rigid termination in molten metal if such a termination is applied to the end of the tube. Moreover, liquid metal also stretches the confining tube boundaries, making it necessary to take into account the local wall response.

The focus of the present paper is a theoretical study of the resonance conditions for a liquid metal column in a small tube. The emphasis is geared toward the two special problems as outlined above. We propose an alternative driving mechanism based on a periodic Lorentz force induced by an external static magnetic field. This force directly acts on the liquid metal in the inner volume of the resonator. Driving frequencies range from several kHz to several tens of kHz. Two resonator types are basically investigated: a quarter wavelength open–closed resonator with rigid termination at one end, and a half-wavelength open–open resonator. Our goal is to calculate the quality factor and the resonant frequency under different operating conditions and then propose the better choice for the resonator construction.

Since the wavelength is always large in comparison with the tube radius, a spatially one-dimensional acoustic model is formulated, which includes different absorption mechanisms. For the second resonator type, a nonlinear model of the inflow–outflow loss becomes necessary to correctly predict the oscillation amplitude. The force distribution analysis involves analytical calculations and simple eigenfunction expansions.

The paper is organized as follows. Section I outlines the problem statement and gives an overview of the material properties. Section II deals with practically achievable spatial force distributions and the corresponding eigenfunction expansion. Section III introduces the linear acoustic theory. A nonlinear extension is considered in Sec. IV and subsequently applied to the second resonator type. Finally, discussion and conclusions are presented in Sec. V.

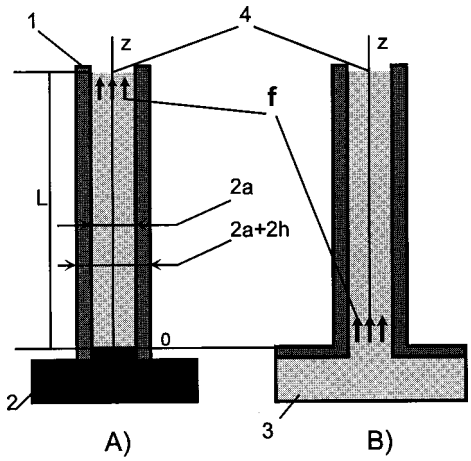

FIG. 1. Geometry of two resonator types. 1—ceramic tube; 2—rigid foundation for the open–closed resonator; 3—outer liquid volume for the open–open resonator; 4—free surface of liquid metal.

I. PROBLEM STATEMENT

The resonator geometry is shown schematically in Fig. 1. Liquid metal fills a cylindrical tube (1) to a column of height L. Tube (1) with inner radius a and outer radius $a+h$ is either closed through a rigid massive foundation (2) or it is connected with an outer liquid volume (3). The upper surface of the liquid column (4) always satisfies the free surface condition by being subjected to an ambient static pressure p_0. The construction shown in Fig. 1 on the left represents a quarter wavelength open–closed resonator (type A) when the melt is driven by a periodic force at its eigenfrequencies. The construction shown in Fig. 1 on the right is a half-wavelength open–open resonator (type B). We will study both types and analyze their performance in terms of quality factor and maximum pressure amplitude.

As a driving force, a distributed Lorentz force density **f** will be analyzed, concentrated mainly in the vicinity of the pressure nodes (Fig. 1) for both resonator types. Only fundamental and second resonance modes are the subject of this study. This approximately yields $L=\lambda/4,3\lambda/4$ for type A, and $L=\lambda/2,\lambda$ for type B. The typical scales under study are $L=50-300\,\mathrm{mm}$, $a=2.5-10\,\mathrm{mm}$, and $h=1-2.5\,\mathrm{mm}$. The liquid metals investigated in this paper are liquid gallium and liquid aluminum.

Since $\lambda \gg a$ is in all situations, a spatially one-dimensional model of resonant acoustic vibration is implemented. The one-dimensional model straightforwardly includes the effect of the finite termination impedance at the tube ends, the effect of thermoviscous sound absorption in the inner tube volume, and the hydrodynamic nonlinearity effect. After some averaging manipulations it is also possible to take into account the effect of wall friction and the effect of locally reacting elastic tube walls.

To get a preliminary estimate of the relative importance of those effects for the acoustic resonator performance, we have collected acoustic and material properties for liquid gallium and liquid aluminum in Tables I and II.[11–17] Necessary

TABLE I. Mechanical and thermal properties of liquid gallium and liquid aluminum near the melting point. For the purpose of comparison, data for water at 20 °C are also presented. The columns denote, respectively, melting point MP in °C of the liquid, density ρ_0, specific heat at constant pressure c_p, ratio of specific heats $\gamma=c_p/c_v$, sound speed c_0, shear viscosity η_s, thermal conductivity κ, sound absorption coefficient α/f^2, effective shear viscosity η_e, and nonlinear parameter of liquid B/A.

	MP, °C	ρ_0, kg/m^3	c_p, J/kg K	c_p/c_v	c_0, m/s	η_s, Pa s	κ, J/m s K	α/f^2, s^2/m	η_e/η_s	B/A
Ga	29.78	6100	400	1.10	2800	0.0021	31	1.6e−15	2.5	3.7
Al	660.2	2400	1100	1.25	4700	0.002	115	2.3e−15	8.9	2.1
H_2O	0	1000	4200	1.0	1480	0.001	0.5	25.0e−15	1.0	5

data on tube and termination materials are given in Table III.[17–19] Among other familiar quantities, the effective shear viscosity

$$\eta_e=\eta_s\left(1+\frac{\beta c_0^2}{c_p}\sqrt{\frac{\kappa}{\eta_s c_p}}\right)^2, \tag{1}$$

is introduced into consideration to study the wall friction effect[20] in the thermoviscous fluid [Ref. 21, p. 209; Ref. 22, Eq. (36)]. This characterizes equivalent increase in shear viscosity while taking into account the temperature boundary layer (cf. Ref. 22). In comparison with a water- or air-filled resonator, the following observations can be made from Tables I–III:

(i) Due to the extremely high acoustic impedance of the liquid metal it is difficult to guarantee high reflectivity from the closed end boundary. The most suitable material for this purpose with largest longitudinal impedance would be probably tungsten or tungsten carbide.

(ii) The same reason makes it necessary to include into consideration the local stiffness and mass response of the tube wall.

(iii) The effect of thermoviscous volume absorption seems to be unimportant in comparison with the acoustic losses due to wall friction.

II. DRIVING FORCE

A. Geometry

A typical situation allows us to consider two current supplying electrodes immersed in the liquid metal in proximity to the tube wall, as is shown in Fig. 2. For simplicity, we have put the origin of a Cartesian coordinate system in the plane of the two electrodes. The external static magnetic field **B** is directed toward the *y*-axis. The Lorentz force density is given by

$$\mathbf{f}=\mathbf{i}\times\mathbf{B}. \tag{2}$$

TABLE II. Physical properties of liquid gallium and liquid aluminum near the melting point. The columns denote, respectively, surface tension of liquid state σ with respect to water (σ_0 at 20 °C), wetting properties, and electric resistivity ρ_l in Ω m.

Metal	σ/σ_0	Wetting	ρ_l, Ω m
Ga	9.7	glass, porcelain	25.9×10^{-8}
Al	13	quartz	26.0×10^{-8}

For our consideration, only the *z*-component of **f**, denoted by *f*, is of interest for the excitation of longitudinal vibrations. From Eq. (2), we obtain

$$f=Bi_x. \tag{3}$$

Quasi-steady[23] current distribution within a finite conducting cylinder is calculated based on the Green's function approach.[24,25] Green's function of a simple current source $q=I\delta(\mathbf{r}-\mathbf{r}_0)$ in the interior of the finite cylinder of height *L* is obtained in terms of cylindrical coordinates r,θ,z in the form (cf. also the corresponding acoustic solutions[26,27])

$$G(\mathbf{r}|\mathbf{r}_0)=I\rho_l\sum_{m=0,n=0,p=0}^{\infty}G_{mnp}H_{mnp}(\mathbf{r})H_{mnp}(\mathbf{r}_0), \tag{4}$$

$$H_{mnp}(\mathbf{r})=J_m(\lambda_{mn}r/a)\cos(m\theta)\cos(\pi pz/L), \tag{5}$$

$$G_{mnp}=\frac{\epsilon_m\epsilon_p}{\pi La^2(1-m^2/\lambda_{mn}^2)(\lambda_{mn}^2/a^2+\pi^2p^2/L^2)J_m^2(\lambda_{mn})}. \tag{6}$$

Here, J_m is the Bessel function of order *m*, λ_{mn} are consecutive zeros of the Bessel function derivative J_m', i.e., $J_m'(\lambda_{mn})=0$, $n=0,1,\ldots$. The Neumann factors ϵ_m, ϵ_p are equal to *l* if *m*, $p=0$ and 2 otherwise. Figure 3 shows the contour plot of the axial current density component i_x, which is proportional to the Lorentz force density, due to two current sources oppositely placed on the wall, along the symmetry plane. The current and the force are well localized near the plane of two electrodes. The width of the localization domain is about one tube radius *a*.

The total Lorentz force *F* in the *z* direction is of primary importance for the oscillation magnitude. It follows from the current conservation law that

$$F=B\int_V i_x\,dx\,dy\,dz=2aIB. \tag{7}$$

B. Eigenfunction expansion

In general, we assume a harmonic current and harmonic driving force, i.e., $I=\hat{I}e^{j\omega t}$, $f=\hat{f}e^{j\omega t}$. A connection should be established between the physically available spatial force distribution and the eigenfunction expansion, used for the theoretical predictions below. The eigenfunction expansion is governed by

TABLE III. Mechanical properties of a range of solid insulators for tube walls and/or tube terminations. For the purpose of comparison, data of the acoustic impedances of liquid gallium and aluminum are also presented. The columns denote, respectively, density ρ_s, Young's modulus E, Poisson's ratio ν, low-frequency phase velocity of compressional waves in a elastic plate c_p, longitudinal impedance $Z_s=\rho_s c_l$, and maximal use temperature, respectively.

Material	ρ_s, kg/m^3	E, Gpa	Poisson's ratio	c_p, m/s	$Z_s=\rho_s c_l$, kg/m^{2}s	Maximal operating temperature, °C
Tungsten carbide (WC)	15 700	700	0.18	6788	1.1e+8	>1000 °C
Tungsten	19 350	375	0.3	4630	1.1e+8	>1000 °C
Friatec-Degussit® alumina ceramics AL-23	3800	380	0.22	10 300	4.1+7	1950
Fused quartz	2200	73	0.17	5850	1.3e+7	1000
Liquid Ga	6100	⋯	⋯	⋯	1.7e+7	⋯
Liquid Al	2400	⋯	⋯	⋯	1.1e+7	⋯

$$f=e^{j\omega t}\sum_{n=1}^{\infty} f_n \sin k_{1n}z, \quad k_{1n}=\left(n-\frac{1}{2}\right)\frac{\pi}{L}, \quad z\in(0,L), \tag{8a}$$

$$f=e^{j\omega t}\sum_{n=1}^{\infty} f_n \cos k_{1n}z, \quad k_{1n}=n\frac{\pi}{L}, \quad z\in(0,L) \tag{8b}$$

for the open–closed or open–open resonator, respectively.

Since $a\ll L$, the axial Lorentz force density, Eq. (3), for the lowest resonances is quite well approximated by a δ-function located in the plane of two electrodes at $z=z_0$, i.e.,

$$\hat{f}=\frac{F}{S}\delta(z-z_0)=\frac{2a\hat{I}B}{S}\delta(z-z_0). \tag{9}$$

We will put $z_0=L-a$ for the open–closed resonator and $z_0=a$ for the open–open resonator, respectively. This gives in the main order with respect to small parameter a/L

$$f_n=\frac{4a\hat{I}B}{SL}(-1)^{n+1} \quad \text{for type A,}$$
$$f_n=\frac{4a\hat{I}B}{SL} \quad \text{for type B.} \tag{10}$$

Due to the orthogonality condition for the corresponding boundary value problem, coefficient f_1 characterizes the fundamental resonance only, coefficient f_2 the second resonance, etc. We restrict ourselves to the fundamental or the second resonance expansion term.[28]

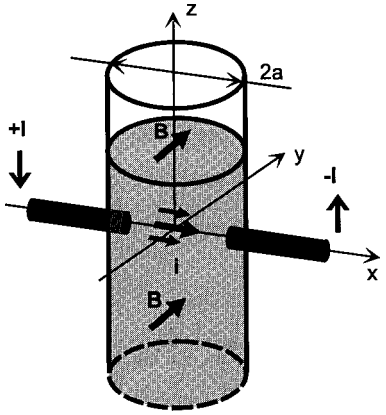

FIG. 2. Two current carrying electrodes and the external magnetic field applied to the liquid metal column.

III. LINEAR ACOUSTIC THEORY

A. Wave equation for the liquid metal

The wave equation for the liquid metal should thus involve the local wall response and the boundary layer effect. If the acoustic pressure stretches the flexible tube so that its radius a becomes $a+\eta$ ($\eta/a\ll 1$), the wave equation is simply obtained from mass and momentum conservation laws in the form (Ref. 29, pp. 688–689)

$$\frac{\partial^2 p}{\partial t^2}-c_0^2\frac{\partial^2 p}{\partial z^2}+c_0^2\frac{2\rho_0}{a}\frac{\partial^2 \eta}{\partial t^2}=0. \tag{11}$$

In Eq. (11), we neglected nonlinearities such as $p\eta$.

The effect of wall friction (long-wavelength limit) results in the substitution[20]

$$\frac{\partial p}{\partial z}\to\left[1-\frac{2}{a}\sqrt{\frac{\mu_e}{j\omega}}\right]\frac{\partial p}{\partial z}, \tag{12}$$

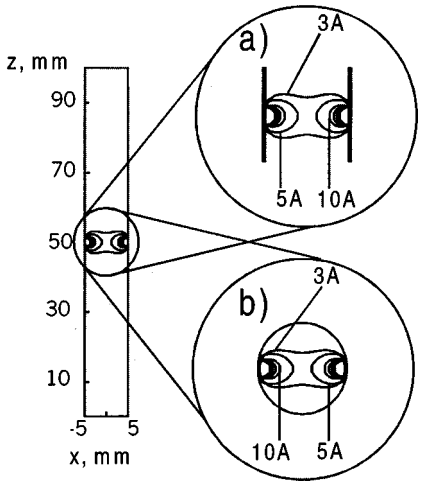

FIG. 3. Contour plot of axial current density i_x for the cylinder of 100 mm in height and 10 mm in width. (a) Axial plane; (b) radial plane. Two point current sources are oppositely placed on the tube wall. The total current is 35 A rms.

which should be made in the momentum equation for a harmonic wave. The continuity equation remains the same. In time domain, such substitution corresponds to the integral operator[30]

$$\frac{\partial p}{\partial z} \rightarrow \frac{\partial p}{\partial z} - \frac{2}{a}\sqrt{\frac{\mu_e}{\pi}}\int_{-\infty}^{t} \frac{\partial p(z,\tau)/\partial z}{\sqrt{t-\tau}}\, d\tau. \tag{13}$$

Equation (11) is then derived in the form:

$$\frac{\partial^2 p}{\partial t^2} - c_0^2\left(\frac{\partial^2 p}{\partial z^2} - \frac{2}{a}\sqrt{\frac{\mu_e}{\pi}}\int_{-\infty}^{t} \frac{\partial^2 p(z,\tau)/\partial z^2}{\sqrt{t-\tau}}\, d\tau\right) + c_0^2 \frac{2\rho_0}{a}\frac{\partial^2 \eta}{\partial t^2} = 0. \tag{14}$$

B. Vibrations of tube walls

The local mass response of the cylindrical tube with wall thickness h is governed by the equation[29,31,32]

$$\frac{\partial^2 \eta}{\partial t^2} - \frac{p}{\rho_s h} = 0, \tag{15}$$

which is a direct consequence of Newton's second law for the tube material under pressure load. The local stiffness response is obtained from Hook's law

$$\rho_s h \frac{\partial^2 \eta}{\partial t^2} = -K\eta. \tag{16}$$

The stiffness of the tube wall K explicitly in terms of tube parameters reads[20,32]

$$K = \frac{h}{a^2}E \text{—nontethered tube}, \qquad K = \frac{h}{a^2}\frac{E}{1-\nu^2} \text{—tethered tube}. \tag{17}$$

We are basically interested here in the nontethered tube, which is mostly free with respect to longitudinal displacements (cf. Fig. 1). Combination of Eqs. (15) and (16) yields

$$\frac{\partial^2 \eta}{\partial t^2} + \frac{K}{\rho_s h}\eta - \frac{p}{\rho_s h} = 0. \tag{18}$$

The mass response is usually of negligibly small contribution in comparison with the stiffness response.[20] However, this can be important in our case for not very hard materials with smaller Young's modulus (fused quartz) at higher frequencies of order 20 kHz.

The bending stress would give a correction

$$c_p^2 \frac{h^2}{12}\frac{\partial^4 \eta}{\partial z^4} \tag{19}$$

into the left-hand side of Eq. (18). This result is obtained from the complete equations for thin shells.[32,33] As compared to other terms in Eq. (18), such a correction is, however, of order h^2/λ^2. In our situation $h^2/\lambda^2 \ll 1$, and the contribution given by Eq. (19) can be neglected.

Equation (18) goes along with the more precise theory of acoustic wave propagation in fluid-filled elastic tubes[34–36] in the low-frequency limit and is originally due to Morse and Ingard (Ref. 29, pp. 688–689). Its more complicated versions with taking into account bending effects are also available from the literature.[33,37]

For the nontethered tube, longitudinal stresses and velocities of the wall material can be shown to be in phase with fluid pressures and velocities.[20] Therefore, they will automatically satisfy the same boundary conditions as those for the liquid metal column. This means no longitudinal stress at the open end and vanishing longitudinal displacement at the closed end (resonator type A). For the combination of a ceramic tube and tungsten termination, this is a rather good approximation to reality.

C. Coupled equations

The coupled equations for the standing wave in the flexible tube, which take into account the acoustic boundary layer effect, are obtained from the two previous subsections in the form

$$\frac{\partial^2 p}{\partial t^2} - c_0^2\left(\frac{\partial^2 p}{\partial z^2} - \frac{2}{a}\sqrt{\frac{\mu_e}{\pi}}\int_{-\infty}^{r} \frac{\partial^2 p(z,\tau)/\partial z^2}{\sqrt{t-\tau}}\, d\tau\right) + c_0^2 \frac{2\rho_0}{a}\frac{\partial^2 \eta}{\partial t^2} = -c_0^2 \frac{\partial f}{\partial z}, \tag{20}$$

$$\frac{\partial^2 \eta}{\partial t^2} + \frac{K}{\rho_s h}\eta - \frac{p}{\rho_s h} = 0. \tag{21}$$

We substitute the expression for the Lorentz force density f from Eqs. (8) of Sec. II, where only the first or the second term on the right-hand sides is retained. This corresponds to the fundamental or second resonant mode, respectively. The boundary conditions for the resonator of type A imply that

$$p(0,t)/w(0,t) = Z_s \quad \text{at } z = 0, \tag{22a}$$

$$p(L,t) = 0 \quad \text{at } z = L. \tag{22b}$$

The acoustic termination impedance Z_s is given for some hard materials in Table III. The boundary conditions for resonator type B in time domain read [cf. Ref. 21, Eq. (9.10)]

$$p(0,t) = -a\rho_0\left(\frac{8}{3\pi}\frac{\partial w(0,t)}{\partial t} - \frac{a}{2c_0}\frac{\partial^2 w(0,t)}{\partial t^2}\right) \quad \text{at } z = 0, \tag{23a}$$

$$p(L,t) = 0 \quad \text{at } z = L. \tag{23b}$$

The expression in Eq. (23a) is the linear radiation condition for the flanged tube open from the bottom into the outer liquid metal volume [cf. Fig. 1(B)].

Two quantities are to be evaluated for the fundamental and second resonance condition: the quality factor of the resonator Q and its resonant frequency Ω. The quality factor is introduced as the ratio of maximum acoustic pressure force SP on the liquid volume divided by the total driving force F_n corresponding to nth resonance (in our case $n = 1,2$). The total driving force is obtained by integration of Eqs. (8) over the entire volume if only one term is kept on the right-hand sides. As the integrand, we consider the absolute value of this term. By taking into account Eqs. (10), this gives $F_n = (2/\pi)LS|f_n| = (8/\pi)a|\hat{I}|B$ $(n = 1,2)$ and

$$Q=\frac{SP}{|F_n|}=\frac{\pi S}{8a|\hat{I}|B}P. \tag{24}$$

D. Solution: Open–closed resonator

The general solution of Eqs. (20) and (21) supplied with the corresponding boundary conditions Eqs. (22) takes the form

$$p=e^{j\omega t}(p_1\cos k_1 z+p_2\sin k_2(z-L)),$$

$$w=e^{j\omega t}\frac{1}{j\omega\rho_0}(k_1p_1\sin k_1z-k_2p_2\cos k_2(z-L)), \tag{25}$$

$$\eta=e^{j\omega t}(\eta_1\cos k_1z+\eta_2\sin k_2(z-L)).$$

Wave number k_1 is always due to the external force, i.e. [see Eq. (8b)], $k_1=\pi/2L,\ 3\pi/2L$ for the fundamental and second resonance, respectively. The free surface boundary condition is satisfied automatically. Five unknown coefficients $p_1, p_2, \eta_1, \eta_2, k_2$ are then found from the differential equations and from the remaining boundary condition. However, we will obtain the solution for each physical mechanism, limiting the resonant amplitude, separately, and then build up a combination of them. Such an approach is widely used in the study of acoustic resonant oscillations with multiple dissipation mechanisms. Furthermore, each physical effect will only be analyzed to the first order of approximation with respect to the corresponding small parameter (frequency shift or energy loss per period).

The effect of flexible tube walls is obtained if we neglect the friction term in Eq. (20) and let $Z_s\to\infty$ in Eq. (22a). This yields $p_2=0,\ \eta_2=0$ in Eq. (25). Simple calculation gives

$$\Omega=c_0k_1\left(1-\frac{\rho_0c_0^2}{a(K-\rho_shc_0^2k_1^2)+2\rho_0c_0^2}\right),\quad Q=\infty \tag{26}$$

at relatively small values of $(\Omega-c_0k_1)/c_0k_1$. Equation (26) states that there is practically no acoustic loss due to the vibrating walls. This seems to be a reasonable assumption for the liquid metal resonator surrounded by air. The effect of the acoustic boundary layer also requires $p_2=0,\ \eta_2=0$. It gives

$$\Omega=c_0k_1\left(1-\sqrt{\frac{\mu_e}{2a^2c_0k_1}}\right),\quad Q=\frac{\pi}{2L}\sqrt{\frac{a^2c_0}{2k_1\mu_e}} \tag{27}$$

to first order of approximation. Finally, the effect of nonrigid termination with zero reactance yields

$$\Omega=c_0k_1,\quad Q=\frac{\pi}{4}\frac{Z_s}{\rho_0c_0}. \tag{28}$$

The resulting resonant frequency is approximately obtained as a sum of those corrections to the unperturbed value c_0k_1. The total quality factor is well approximated by the inverse of the sum of inverse quality factors, i.e.,[38]

$$\Omega=c_0k_1+\sum_m(\Omega_m-c_0k_1),\quad Q=\frac{1}{\Sigma_mQ_m^{-1}}. \tag{29}$$

The analysis of physical conditions presented in Tables I and III indicates that the main mechanism, responsible for damping the resonant oscillations, will be the relatively low termination impedance, even if hard materials like tungsten or tungsten carbide are used. To illuminate this conclusion, Fig. 4 presents the quality factors given by Eqs. (27) and (28), respectively, as a function of height L of the liquid metal column. The fundamental resonance is studied for a tube filled with liquid gallium, assuming a tungsten or tungsten carbide termination. Nearly the same results are obtained for the tube filled with molten aluminum.

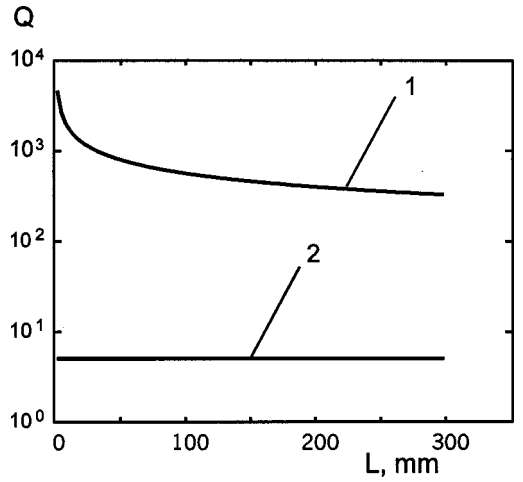

FIG. 4. Quality factor of the open–closed resonator (liquid gallium) as a function of height L of the liquid metal column at $a=5$ mm. 1—effect of the boundary layer losses; 2—effect of the finite termination impedance (tungsten or tungsten carbide).

To get some absolute estimates of achievable pressure amplitudes, a driving source has to be specified. Let us consider a commercially available ac high-current sinusoidal generator with the current amplitude of 50 A (35-A rms). If this current flows through the liquid metal subjected to an external static magnetic field about 1 Tesla (cf. Fig. 2) then the amplitude of the Lorentz force Eq. (7) appears of 0.5 N ($a=5$ mm).[39] (The magnetic-acoustic interaction[39] is assumed to be negligibly small.) The total driving force F_n corresponding to the nth resonance from Eq. (24) is somewhat larger and it is about 0.64 N ($n=1,2$). This value divided by the tube cross-section (0.78 cm^2 at $a=0.5$ cm) and multiplied by Q (say 5) gives us a pressure oscillation amplitude of 0.4 atm. It is probably too low to expect a considerable practical application of this resonator type. Compared with internal pressures $\rho_0c_0^2/(B/A+1)$ for the liquid metals, it is also too low for any nonlinear effects.

E. Solution: Open–open resonator

The general solution again has the form of Eq. (25) but $\cos k_1z$ is replaced by $\sin k_1z$, $\sin k_1z$ is replaced by $-\cos k_1z$; $k_1=\pi/L,\ 2\pi/L$ for the fundamental and second resonance, respectively. The effect of flexible tube walls and that of acoustic boundary layers are, as before, given by Eqs. (26) and (27), respectively. However, the radiation boundary condition (23a) for the flanged tube yields

$$\Omega=c_0k_1\left(1-\frac{8}{3\pi}\frac{a}{L}\right),\quad Q=\frac{\pi}{2}\frac{1}{(k_1a)^2} \tag{30}$$

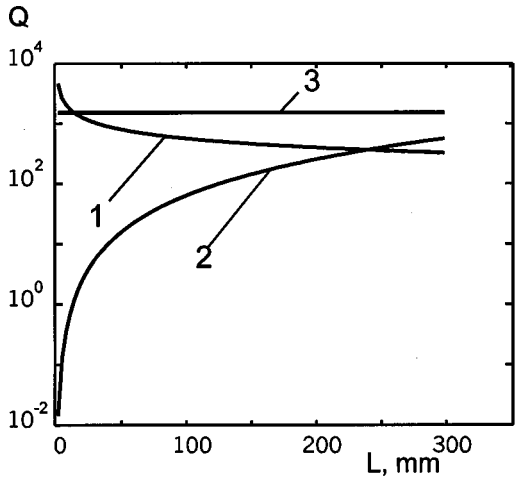

FIG. 5. Quality factor of the open–open resonator (liquid gallium) as a function of height L of the liquid metal column at $a=5$ mm. 1—effect of the boundary layer losses; 2—effect of open-end acoustic losses (linear theory); 3—effect of open-end hydrodynamic losses (nonlinear theory, $F_n=0.64$ N).

instead of Eq. (28). The resonant frequency agrees to main order with the calculation for the piston-driven acoustic resonator (Ref. 21, p. 202) if the driver presents a vanishing mechanical impedance. Figure 5 shows the quality factors given by Eqs. (27) and (30), respectively, as a function of height L of the liquid metal column. The resulting quality factor appears, in general, much greater than the quality factor for the open–closed resonator, but as L is considerably greater than the tube cross-section.

We check here the example given at the end of previous subsection and assume the same driving force of 0.64 N. For the open–open resonator, the pressure oscillation amplitude reaches 12.7 atm already for a tube with $a=5$ mm and $L=200$ mm, if the fundamental resonance is considered.

IV. NONLINEAR ANALYSIS

It is well known from both theory and experiment for open tubes that Eqs. (27) and (30) overestimate the quality factor at high oscillation amplitudes, whereas, at small amplitudes, they are close to reality.[40] The reason for such disagreement is the nonlinearity of the hydrodynamic flow, which drastically reduces the oscillation amplitude. For open resonators, there are two sources of nonlinearity: the nonlinearity of the flow within the tube and the boundary condition nonlinearity. The latter appears due to boundary layer separation from the tube wall at outflow (inflow), which is basically more important[40–43] than the familiar nonlinear distortion in the inner volume.

We apply the following nonlinear boundary condition[40] replacing Eq. (23a):

$$p(0,t)=-\rho_0\alpha|w(0,t)|w(0,t) \quad \text{at } z=0, \tag{31}$$

where α is a numerical factor on the order of unity. This type of nonlinear boundary condition is also known as Bernoulli's loss. Disselhorst and van Wijngaarden[40] discuss $\alpha=0$ at outflow and $\alpha=0.5$ or 1 at inflow for an unflanged tube with round or sharp edges, respectively. For the final result, it does not matter whether α is a step function or a constant: only its time-averaged value over a wave period is significant. Therefore, we set α to be a constant everywhere. Physically, this means an equal loss distribution between inflow and outflow.

Further treatment follows the standard template of nonlinear acoustics[44,45] (see also Refs. 30, 46). Dimensionless wave amplitude plays the role of a small but finite parameter. The flow in the tube is divided into forward p^+,w^+ and reverse p^-,w^- traveling waves, i.e.,

$$\begin{aligned} &p=p^++p^-, \quad w=w^++w^-,\\ &p^+=\rho_0c_0w^+, \quad p^-=-\rho_0c_0w^-. \end{aligned} \tag{32}$$

The real part of the force expansion Eq. (8b) (we assume for simplicity that $\mathrm{Im}\{f_n\}=0$) may be cast for the fundamental and the second resonance in the form

$$\begin{aligned} \mathrm{Re}\{f_ne^{j\omega t}\cos k_{1n}z\}&=\tfrac{1}{2}f_n\cos\omega(t-z/c_0)\\ &\quad+\tfrac{1}{2}f_n\cos\omega(t+z/c_0), \end{aligned} \tag{33}$$

where we have substituted $k_{1n}\cong\omega/c_0$ at resonance. Applying the multiple-scale asymptotic technique to the hydrodynamic equations of motion, it can be shown that both elementary traveling waves should satisfy the inhomogeneous simple wave equation (cf. Ref. 45)

$$\frac{\partial w^\pm}{\partial z}-\frac{n+1}{2c_0^2}w^\pm\frac{\partial w^\pm}{\partial\tau}=\pm\frac{f_n}{4\rho_0c_0}\cos\omega\tau \tag{34}$$

to second order. Here, $\tau=t\mp z/c_0$ is the retarded time. Equation (34) ignores the interaction between two oppositely directed waves. Fortunately, the nonlinear interaction between two counterpropagating waves is not cumulative over one period and contributes finally only a third-order correction.[47]

Substituting Eq. (32) into Eq. (31) and Eq. (23b), one obtains

$$\begin{aligned} w^+(0,\tau)-w^-(0,\tau)=&-\frac{\alpha}{c_0}|w^+(0,\tau)+w^-(0,\tau)|(w^+(0,\tau)\\ &+w^-(0,\tau)), \end{aligned} \tag{35a}$$

$$w^+(L,\tau)-w^-(L,\tau)=0. \tag{35b}$$

On the right-hand side of Eq. (35a) we can replace $w^-(0,\tau)$ by $w^+(0,\tau)$ to first order. This gives

$$w^+(0,\tau)-w^-(0,\tau)=-\frac{4\alpha}{c_0}|w^+(0,\tau)|w^+(0,\tau), \tag{36a}$$

$$w^+(L,\tau)-w^-(L,\tau)=0. \tag{36b}$$

Expansion into a Taylor's series and using Eqs. (34) yields

$$\begin{aligned} w^\pm(L,\tau)&=w^\pm(0,\tau)+L\frac{\partial w^\pm}{\partial z}(0,\tau)\\ &=w^\pm(0,\tau)+\frac{n+1}{2c_0^2}Lw^\pm(0,\tau)\frac{\partial w^\pm(0,\tau)}{\partial\tau}\\ &\quad\pm L\frac{f_n}{4\rho_0c_0}\cos\omega\tau. \end{aligned} \tag{37}$$

If we substitute this expression into Eq. (35b), the following relation is obtained ($\tau=t\mp z/c_0=t$ at $z=0$):

$$w^+(0,\tau)-w^-(0,\tau)=-\frac{n+1}{4c_0^2}L\frac{\partial}{\partial\tau}(w^{+^2}(0,\tau)-w^{-^2}(0,\tau))$$

$$-L\frac{f_n}{2\rho_0 c_0}\cos\omega\tau. \tag{38}$$

It is worth noting that the nonlinearity of the flow within the tube is represented by the first term on the right-hand side of Eq. (38). This term is cancelled to second order since we set $w^-(0,\tau)=w^+(0,\tau)$ to main order. Exactly the same is valid for the nonlinear correction to the two familiar expressions $p^+=\rho_0 c_0 w^+$, $p^-=-\rho_0 c_0 w^-$ from Eq. (32). Equation (38) is thus reduced to

$$w^+(0,\tau)-w^-(0,\tau)=-L\frac{f_n}{2\rho_0 c_0}\cos\omega\tau. \tag{39}$$

We see that the flow nonlinearity for open resonators only appears as a third-order effect[42,48] which is beyond the scope of our analysis. However, the boundary condition nonlinearity appears to second order already. Substitution of Eq. (39) into Eq. (36a) yields

$$w^+(0,\tau)=\frac{1}{2}\sqrt{\frac{Lf_n}{2\rho_0\alpha}}\sqrt{|\cos\omega\tau|}\,\mathrm{sgn}(\cos\omega\tau). \tag{40}$$

To within a constant factor, Eq. (40) coincides with the well-known van Wijngaarden's solution for the piston-driven acoustic resonator.[42,40]

Using Eq. (32), the maximum pressure amplitude P is found at antinodes

$$P\cong 2\rho_0 c_0 \max(w^+(0,\tau))=\sqrt{L\rho_0 c_0^2 f_n/2\alpha}. \tag{41}$$

The quality factor Eq. (24) is now calculated as follows:

$$Q=\frac{\pi}{4}\sqrt{\frac{2\rho_0 c_0^2}{\alpha L f_n}}=\frac{\pi}{2}\sqrt{\frac{\rho_0 c_0^2 a^2}{\alpha F_n}}. \tag{42}$$

The second expression involves the total resonance force F_n applied to the liquid metal volume. We have taken $\alpha=2$ in Eq. (42) to obtain the upper limit of the inflow–outflow losses and to account for experimentally observed additional losses (cf. Ref. 40).

Figure 5 plots the values of the quality factor Eq. (42) as a function of height L of the liquid metal column. Also shown are the quality factors predicted by the linear theory. In each case, the total driving force is 0.64 N (cf. example in previous section). For a 200-mm-long metal column ($a=5$ mm), the oscillation amplitude decreases from 12.7 to 11.5 atm due to the nonlinearity [the total quality factor Eq. (29) decreases by 10%]. This still represents a reasonably small correction. However, the nonlinear saturation effect increases rapidly with increasing oscillation amplitude.

V. DISCUSSION AND CONCLUSIONS

Figure 6 presents the contour plot of the maximum oscillation amplitude P (atm) for the open–open resonator (liquid gallium) as a function of height L of the liquid metal column and tube radius a. The total driving force takes the standard value of 0.64 N. Wall friction, acoustic radiation from the open end, and hydrodynamic inflow–outflow losses

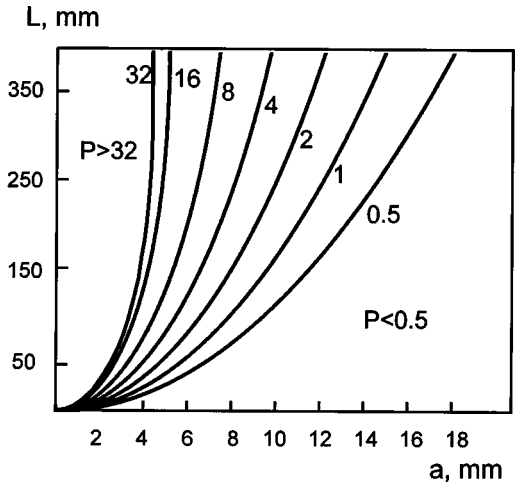

FIG. 6. Contour plot of maximum oscillation amplitude P (atm) for the open–open resonator (liquid gallium) as a function of height L of the liquid metal column and tube radius a. The total driving force is 0.64 N.

are simultaneously taken into account. We can see that this resonator is most effective at rather small tube radii of 2–4 mm. This conclusion is based on the nature of the acoustic and hydrodynamic open-end losses, which strongly depend on the tube radius.

One way to improve the resonator performance would be the use of a flattened rectangular tube under the assumption that the length of the cross-sectional rectangle is considerably greater than its width. Since the alternating current (cf. Sec. II) is allowed to flow along the larger rectangle side, the current path and the total force increase proportional to the side length. For example, if a rectangular tube with side ratio 1:4 is considered instead of a circular tube of the same cross-section, the total Lorentz force Eq. (7) becomes $\sqrt{\pi}\approx 1.8$ times larger. The radiation loss remains the same since it depends on the tube cross-section only. The boundary layer loss increases slightly depending on the cross-section perimeter.

Notice that the periodic current source is accompanied by a periodic Joule's heat source in the plane of two electrodes. The heat source itself can induce resonant oscillations much as periodic laser heating does in a resonance tube terminated by IR transparent windows.[49] In this case, we do not need the external magnetic field and the resulting Lorentz force. However, for good conductors, the heat source is estimated to be rather weak as a practical way of generating high-power resonance oscillations.

An important question beyond the scope of this paper is the effect of surface tension of the liquid metal on its free surface and the wetting effect of the tube wall on the quality factor of the resonator. We believe that, under presence of an acoustic field, there should be good wetting contact for liquid gallium and aluminum residing in quartz or ceramic tubes with weak surface roughness.

The following theoretical conclusions can be drawn based on the studies conducted in this paper:

(i) The resonant oscillation of a relatively small liquid metal column over a wide range of frequencies (5–40 kHz) can be excited by alternating Lorentz forces applied directly to the liquid metal.

(ii) The best performance is achieved for the open-open, half-wavelength resonator of circular or elongated cross-section. The presence of a rigid termination (open–closed quarter wavelength resonator) drastically reduces the quality factor of this resonator.

(iii) For the current of 35 A rms, pressure amplitudes of 10–20 atm can be expected at resonant oscillations in the frequency range of 5–40 kHz. Those conclusions are primarily related to liquid metal with rather high conductivity (liquid gallium or aluminum). Otherwise, Joule's heating plays an important role and additionally must be taken into consideration. Indeed, if the resonant tube is terminated by a local mechanical mass-spring system (for example, membrane fixed at the rim), then large pressure amplitudes can be obtained for the open–closed resonator as well. However, they are restricted to certain fixed eigenfrequencies.

[1] L. Bergmann, *Ultrasonics and Their Scientific and Technical Applications*, 3rd rev. ed. (United States Bureau of Ships, Washington, D.C., 1951).

[2] T. L. Tolt and D. L. Feke, ''Separation of dispersed phases from liquids in acoustically driven chambers,'' J. Chem. Eng. Sci. **48**, 527–540 (1993).

[3] R. E. Apfel, ''Sonic effervescence: A tutorial on acoustic cavitation,'' J. Acoust. Soc. Am. **101**, 1227–1237 (1997).

[4] G. I. Eskin, *Ultrasonic Treatment of Light Alloy Melts* (Gordon and Breach, Amsterdam, The Netherlands, 1998), Chaps. 2, 3.

[5] S. Asai, ''Recent activities on electromagnetic processing of materials,'' in *Proceedings of The Julian Szekely Memorial Symposium on Material Processing*, edited by H. Y. Sohn, J. W. Evans, and D. Apelian (Minerals, Metals & Materials Soc., Warrendale, PA, 1997), pp. 301–311.

[6] D. Apelian, ''Advances in metal treatment of aluminum and foundry alloys,'' in *Proceedings of the International Symposium on Light Metals 1997 Métaux Légers*, edited by C. M. Bickert and R. I. L. Guthrie (Canadian Institute of Mining, Metallurgy and Petroleum, Montreal, 1997), pp. 117–139.

[7] P. Pouly and E. Wuilloud, ''On the efficiency of in-line devices to clean the melt,'' in *Light Metals 1997*, edited by R. Huglen (The Minerals, Metals & Material Soc., Warrendale, PA, 1997), pp. 829–835.

[8] C. E. Eckert, ''Apparatus and method for ultrasonic detection of inclusions in molten metals,'' U.S. Patent 4,563,895 (1986).

[9] N. D. G. Mountford, I. D. Sommerville, A. Simeonescu, and C. Bai, ''Sound pulses enable the online visualization of liquid metal quality,'' in *Proceedings of the International Symposium on Light Metals 1997 Métaux Légers*, edited by C. M. Bickert and R. I. L. Guthrie (Canadian Institute of Mining, Metallurgy and Petroleum, Montreal, 1997), pp. 197–211.

[10] R. C. Stiffler, R. C. Wojnar, M. F. A. Warchol, L. W. Cisko, and J. M. Urbanic, ''Apparatus and method for ultrasonic particle detection in molten metal,'' U.S. Patent 5,708,209 (1998).

[11] R. T. Smith, G. M. B. Webber, F. R. Young, and R. W. B. Stephens, ''Sound propagation in liquid metals,'' in *The Properties of Liquid Metals*, edited by P. D. Adams, H. A. Davies, and S. G. Epstein (Taylor & Francis, London, 1967), pp. 515–522.

[12] G. M. B. Webber and R. W. B. Stephens, ''Transmission of sound in molten metals,'' in *Physical Acoustics*, Vol. IV-B, edited by W. P. Mason (Academic, New York, 1968), pp. 53–97.

[13] J. E. Hatch, Ed., *Aluminum: Properties and Physical Metallurgy* (American Society for Metals, Metals Park, OH, 1984), Chap. 1.

[14] T. Iida and R. I. L. Guthrie, *The Physical Properties of Liquid Metals* (Clarendon, Oxford, 1988).

[15] R. I. L. Guthrie, *Engineering in Process Metallurgy*, 2nd ed. (Clarendon, Oxford, 1992).

[16] G. T. Dyos and T. Farrell, Eds., *Electrical Resistivity Handbook* (Peter Peregrinus, London, 1992).

[17] I. S. Grigoriev, E. Z. Meilikhov, and A. A. Radzig, Eds., *Handbook of Physical Quantities* (CRC, Boca Raton, 1997).

[18] S. W. H. Yih and C. T. Wang, *Tungsten: Sources, Metallurgy, Properties, and Applications* (Plenum, New York, 1979).

[19] E. A. Almond, ''Deformation characteristics and mechanical properties of hard metals,'' in *Science of Hard Materials*, edited by R. K. Viswanadham, D. J. Rowcliffe, and J. Gurland (Plenum, New York, 1983), pp. 515–557.

[20] M. J. Lighthill, *Waves in Fluids* (Cambridge U.P., Cambridge, 1978).

[21] L. E. Kinsler, A. R. Frey, A. B. Coppens, and J. V. Sanders, *Fundamentals of Acoustics*, 3rd ed. (Wiley, New York, 1982).

[22] S. Makarov and E. Vatrushina, ''Effect of the acoustic boundary layer on a nonlinear quasiplane wave in a rigid-walled tube,'' J. Acoust. Soc. Am. **94**, 1076–1083 (1993).

[23] The term ''quasi-steady'' relies on the electromagnetic field. This means that we still calculate the current using an electrostatic solution (Laplace equation) multiplied by the periodically oscillating time factor. Otherwise, Maxwell equations should be solved to calculate the unsteady current distribution, which is not a very straightforward task. The background for such an assumption is the inequality $(a/\delta)^2 \ll 1$, where $\delta = \sqrt{2\rho_l/(\mu\omega)}$ is the skin depth layer in the liquid metal; $\mu \approx \mu_0 = 4\pi\,10^{-7}$ Wb/(A m) is the magnetic permeability. At $f = 10$ kHz, $\sigma \approx 2.6$ cm in liquid gallium or aluminum, which certainly applies for the quasi-steady solution, if tube radius does not exceed 1 cm.

[24] P. M. Morse and H. Feshbach, *Methods of Theoretical Physics* (McGraw-Hill, New York, 1953), Vol. I, Vol. II (§ 10.3, p. 1263).

[25] W. R. Smythe, *Static and Dynamic Electricity*, 3rd ed. (McGraw-Hill, New York, 1967, 1968).

[26] Y.-H. Kim and S.-W. Kang, ''Green's solution of the acoustic wave equation for a circular expansion chamber with arbitrary locations of inlet, outlet port, and termination impedance,'' J. Acoust. Soc. Am. **94**, 473–490 (1993).

[27] E. G. Williams, ''On Green's functions for a cylindrical cavity,'' J. Acoust. Soc. Am. **102**, 3300–3307 (1997).

[28] Each term of the eigenmode expansion, Eq. (8), for the driving force contributes to the acoustic pressure in the tube. However, the magnitude of the contribution appears very different depending on the wave number of the mode k_{1n}. If $\omega/c_0 \approx k_{1n}$ then the nth eigenmode satisfies the resonance condition; all other modes are out of resonance. The repetition of the calculation below for a single nonresonant mode indicates that its contribution to the resulting pressure is at least Q times smaller (Q is the quality factor of the resonator) than the contribution of the resonant mode. Since we only consider the fundamental or second resonance, all nonresonant modes are of higher order. This additionally reduces the contributing pressures due to increased damping. As a result, we expect the total contribution of the nonresonant modes to be on the order of $1/Q$ as well. Precise calculations made for a test case (the wall friction is the only absorption mechanism) confirm this conclusion.

[29] P. M. Morse and K. U. Ingard, *Theoretical Acoustics* (McGraw-Hill, New York, 1968).

[30] S. Makarov and M. Ochmann, ''Nonlinear and thermoviscous phenomena in acoustics, Part II (a review),'' Acustica **83**, 197–223 (1997).

[31] P. M. Morse and K. U. Ingard, ''Linear acoustic theory,'' in *Encyclopedia of Physics. Volume XI/l Acoustics I*, edited by S. Fluegge (Springer-Verlag, Berlin, 1961), pp. 44–56, 119–121.

[32] M. C. Junger and D. Feit, *Sound, Structures, and Their Interaction* (MIT Edward Brothers, Cambridge, MA, 1972).

[33] H. Kraus, *Thin Elastic Shells* (Wiley, New York, 1967).

[34] T. C. Lin and G. W. Morgan, ''Wave propagation through fluid contained in a cylindrical, elastic shell,'' J. Acoust. Soc. Am. **28**, 1165–1176 (1956).

[35] M. El-Raheb, ''Acoustic propagation in finite length elastic cylinders. Part I: Axisymmetric excitation,'' J. Acoust. Soc. Am. **71**, 296–306 (1982).

[36] L. D. Lafleur and F. D. Shields, ''Low-frequency propagation modes in a liquid-filled elastic tube waveguide,'' J. Acoust. Soc. Am. **97**, 1435–1445 (1995).

[37] V. E. Nakoryakov, B. G. Pokusaev, and I. R. Shreiber, *Wave Propagation in Gas–Liquid Media* (CRC, Boca Raton, 1993).

[38] Regarding the first equality in Eq. (29), this is a trivial consequence of the perturbation theory. The second equality is more questionable. It was proved to be an asymptotically precise result if the different quality factors have considerably different magnitudes. In the following, exactly this situation will be studied. However, if the magnitudes are the same, Eq. (29) is only an approximation whose error might be on the order of 100%.

[39] Y. Shapira, ''Acoustic wave propagation in high magnetic fields,'' in *Physical Acoustics*, Vol. 5, edited by W. P. Mason (Academic, New York, 1968), pp. 1–58.

[40] H. M. Disselhorst and L. van Wijngaarden, ''Flow in the exit of open pipes during acoustic resonance,'' J. Fluid Mech. **99**, 293–319 (1980).

[41] U. Ingard and H. Ising, ''Acoustic nonlinearity of an orifice,'' J. Acoust. Soc. Am. **42**, 6–17 (1967).

[42] L. van Wijngaarden, ''On the oscillations near and at resonance in open pipes,'' J. Eng. Math. **2**, 225–240 (1968).
[43] R. G. Galiullin, A. Z. Murzakhanova, and I. P. Revva, ''Influence of absorption on the nonlinear oscillations of a gas in a pipe open at one end,'' Sov. Phys. Acoust. **36**, 545–547 (1990).
[44] O. V. Rudenko and S. I. Soluyan, *Theoretical Foundations of Nonlinear Acoustics* (Consultants Bureau, New York, 1977).
[45] V. E. Gusev, ''Build-up of forced oscillations in acoustic resonators,'' Sov. Phys. Acoust. **30**, 121–125 (1984).
[46] S. Makarov and M. Ochmann, ''Nonlinear and thermoviscous phenomena in acoustics, Part I (a review),'' Acustica **82**, 579–606 (1996).
[47] B. R. Seymour and M. P. Mortell, ''Nonlinear resonant oscillations in open tubes,'' J. Fluid Mech. **60**, 733–749 (1973).
[48] M. Ochmann and S. Makarov, ''Nonlinear and thermoviscous phenomena in acoustics, Part III (a review),'' Acustica **83**, 827–844 (1997).
[49] R. Raspet, B. Denardo, H. E. Bass, J. Brewster, and J. Kordomenos, ''Investigation of parametric drive of a longitudinal gas-filled resonance tube,'' J. Acoust. Soc. Am. **99**, 725–729 (1996).